THE ROYAL SOCIETY

Liquid crystals and flow elongation in a spider's silk production line

D. P. Knight[1] **and F. Vollrath**[1,2*]

[1]*Department of Zoology, Universitetsparken B135, Aarhus C, DK 8000, Denmark*
[2]*Department of Zoology, South Parks Road, Oxford OX1 3PS, UK*

Our observations on whole mounted major ampullate silk glands suggested that the thread is drawn from a hyperbolic die using a pre-orientated lyotropic liquid crystalline feedstock. Polarizing microscopy of the gland's duct revealed two liquid crystalline optical textures: a curved pattern in the feedstock within the ampulla of the gland and, later in the secretory pathway, the cellular texture previously identified in synthetic nematic liquid crystals. The behaviour of droplet inclusions within the silk feedstock indicated that elongational flow at a low shear rate occurs in the gland's duct and may be important in producing an axial molecular orientation before the final thread is drawn. Our observations suggested that the structure of the spider's silk production pathway and the liquid crystalline feedstock are both involved in defining the exceptional mechanical properties of spider dragline silk.

Keywords: biopolymer; mesophase; transition; drawing; filament

1. INTRODUCTION

The dragline silks of spiders of the genus *Nephila* have become the benchmarks for silk studies because of their great toughness and tensile strength (Kaplan *et al.* 1994; Vollrath *et al.* 1996). Liquid crystallization probably helps to account for these remarkable properties and a cholesteric liquid crystal phase has been identified in the silk feedstock within the proximal part of the major ampullate gland which secretes dragline silk (Kerkam *et al.* 1991; Willcox *et al.* 1996). However, there are no previous reports on the existence of large-scale, liquid crystalline textures in this material. This is crucial for a full understanding of the spider's remarkable extrusion system with its chemical (Vollrath *et al.* 1998) and physical treatment (Kerkam *et al.* 1991; Willcox *et al.* 1996) of the nascent silk. Here, we present evidence for two large-scale textures in the major ampullate feedstock as it passes through the ampulla and spinning duct of the golden silk spider *Nephila edulis*. We also present evidence that elongational flow occurs as the liquid crystalline feedstock converges within the duct's hyperbolic lumen.

2. MATERIAL AND METHODS

Adult female *N. edulis* with abdomens 14–18 mm in length were fixed by gentle perfusion (30 min at 4 °C) and immersion (3–12 h) in a modified Karnovsky fixative immediately after at least 4 m of silk had been drawn artificially at *ca.* 100 mm s^{-1}. The fixative contained final concentrations of 2% glutaraldehyde, 2% formaldehyde, 0.1 M sodium cacodylate, 0.01 M calcium chloride and 0.35 M sodium chloride and was adjusted to pH 7.4 with hydrochloric acid. After fixation, glands were dissected out in the same buffer and mounted whole in Farrant's gum. This largely abolishes the form birefringence seen in the epithelium and cuticle in uncleared glands, enabling examination of the strong intrinsic birefringence of the silk feedstock within the lumen. Changing the pH of the fixative between 4.5 and 8.5 did not appear to influence the pattern of molecular orientations. Vector plots showing the slow axis and the approximate strength of the retardation were prepared as follows. A Zeiss polarizing microscope was used with a 1λ wave plate set at the unconventional angle of 7° to the analyser to increase the saturation of interference colours produced by relatively weakly birefringent samples. A high resolution colour video camera was attached to the microscope. A matrix of pixels was rotated over the image on a visual display unit at the same rate as the stage was rotated. The orientation at which each pixel gave the strongest blue hue was noted while a subjective estimate of the intensity of the hue gave a rough approximation of the retardation. This is a manual modification of the method described by Newton *et al.* (1995).

Measurements were made with an eyepiece graticule. Curves were fitted using GraphPad Prism v. 2.01 or Excel v. 7.0.

3. RESULTS

The structure of the major ampullate gland in *N. edulis* is shown in figure 1*a*. The glandular secretory portion is divided into two transverse zones, A and B. The term 'ampulla' is used here for the distal part of the secretory portion running from the penultimate bend to its distal end. The ampulla passes its secretion into a truncated conical structure we have termed 'the funnel', which marks the start of a highly elongated, progressively narrowing duct. This duct is folded back on itself in an elongated 'S' to give three limbs (first, second and third). The S-shaped duct terminates in a structure termed 'the valve' (Wilson 1962*a*,*b*, 1969). A short terminal duct runs from the valve to the spigot.

*Author for correspondence (vollrath@biology.aau.dk).

Received 9 November 1998 *Accepted* 17 November 1998

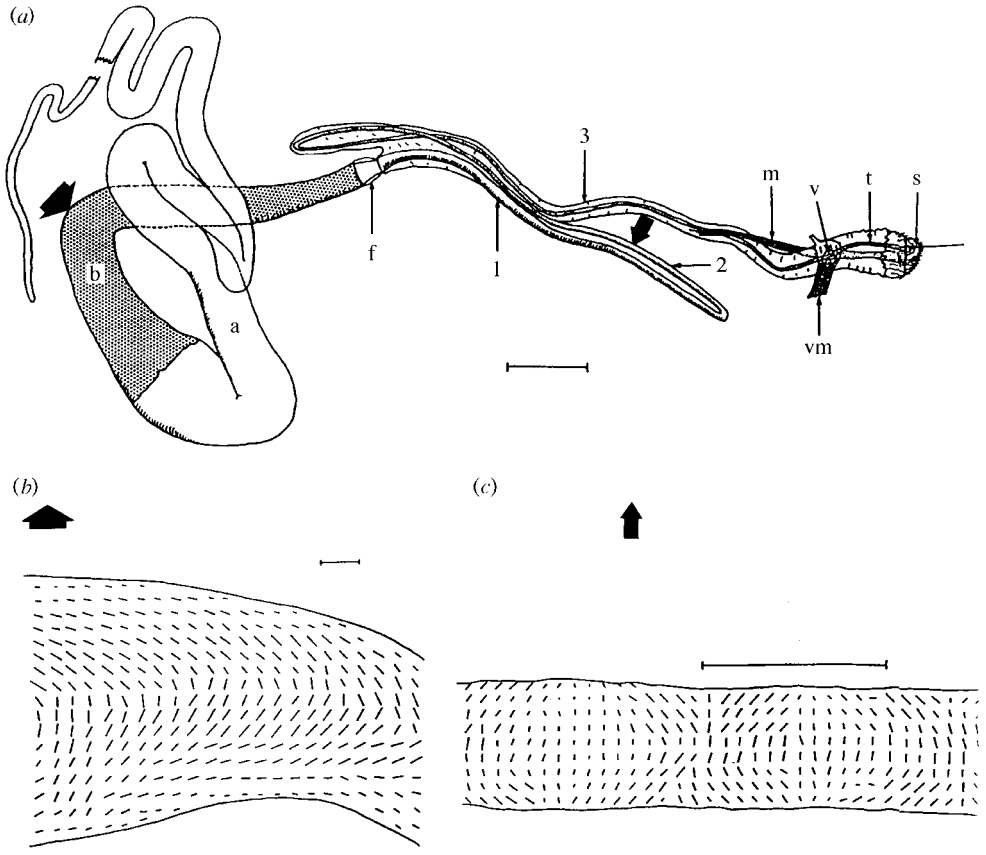

Figure 1. Anatomy of the major ampullate gland in *N. edulis* and vector plots obtained by polarizing microscopy showing the molecular orientation in the feedstock *in situ* at two locations in the gland. The direction of each vector line shows the orientation of the mean slow axis while the length of the line is approximately proportional to the retardation. Broad and narrow arrows mark the approximate location of areas used for figures 1*a* and 1*b*, respectively. (*a*) Drawing of a dissected major ampullate gland taken from a light micrograph. a, zone A; b, zone B; f, funnel; 1, 2 and 3, first, second and third limbs of duct; m, duct levator muscle; v, valve; vm, valve tensor; t, terminal tubule; s, spigot. Scale bar 1 mm. (*b*) Vector plot from a cleared whole mount of the ampulla close to the bend in zone B (see figure 1*a*). The direction of bulk flow was from left to right. A broad arrow indicates location in figure 1*a*. The pattern of nested arcs may arise by elongational flow or bending of a nematic liquid crystal within the divergent–convergent geometry of the ampulla. Scale bar 100 μm. (*c*) As figure 1*b* but showing the cellular texture (see also figure 2) in the feedstock within the second limb of the duct indicated by the arrow in figure 1*a*. Scale bar 100 μm.

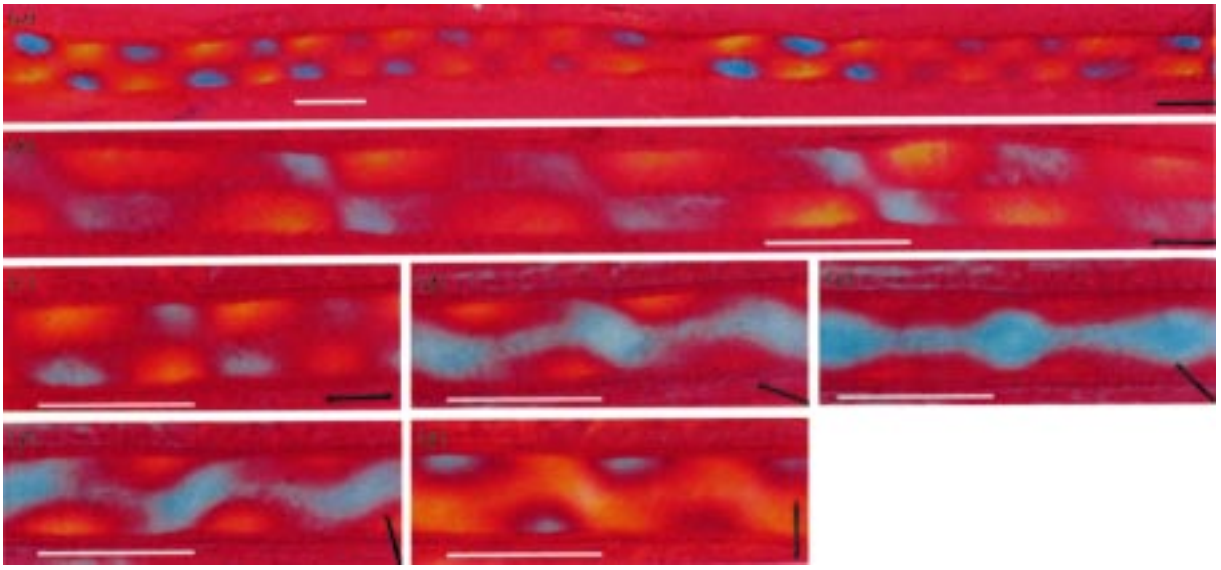

Figure 2. (*a–g*) Polarizing micrographs with 1λ wave plate of cleared whole mounts of similar regions to those used to prepare the vector plot shown in figure 1*c*. The slow axis of the polarizer is indicated by a bar at the bottom right of each micrograph. Scale bar throughout 100 μm. (*c–g*) The effects of rotation of the specimen on the stage of the polarizing microscope.

Polarizing microscopy of whole mounts of aldehyde-fixed glands was used to study the development of molecular orientation in the secretory pathway. A vector plot of the orientation of the slow axes and approximate strength of the retardation of the feedstock in the lumen of the ampulla showed a pattern of nested curves (figure 1*b*). Further down the secretory pathway, feedstock in the lumen of the second limb of the duct frequently showed a different and remarkable large-scale texture (figure 2*a*–2*g*). This consisted of a chequered pattern of rather regularly alternating, approximately rectangular, blue and yellow areas when viewed with a first-order red compensator with the ducts arranged at 0° or 90° to the axis of the polarizer. This optical texture, when rotated between crossed polars (figure 2*a*–2*g*), closely resembled the cellular texture described by Bunning & Lydon (1996) in a synthetic lyotropic nematic discotic (N_D) liquid crystal confined within a narrow cylindrical glass tube. These authors' plot of the disc-shaped bilaminar micelles in their material is practically identical to our plot of the slow axes of the birefringence in the silk feedstock (figure 1*c*). The mean repeat period of the pattern within the silk feedstock in the second limb of the duct was $124 \pm 18\,\mu m$ ($n = 50$). The pattern sometimes started in the distal part of the first limb of the duct and continued into the proximal part of the third limb but showed a longer repeat period in these locations. Later in the third limb, but well before the start of the draw down taper (see below), the silk feedstock usually showed strong positive birefringence with respect to the duct and a relatively sharp extinction indicating a predominantly uniaxial molecular orientation.

Information concerning the rheology of the system was obtained by studying the change in diameter of the lumen along the length of the S-shaped duct. A two-stage hyperbolic curve fitted this closely ($R^2 = 0.979$; see figure 3*a*).

The behaviour of small droplets in the feedstock enabled us to obtain further evidence of elongational flow in the secretory pathway. These droplets appear to give rise to the highly elongated, fine canaliculi described by Frische *et al.* (1997) in the final silk. Feedstock in the centre of the lumen in of the widest part of the ampulla contained spherical droplets of $2.2 \pm 0.49\,\mu m$ ($n = 32$) in diameter surrounded by the bulk phase, a homogeneous matrix. Moving distally through zone B, the shape and size of the droplets in the centre of the lumen did not appear to change significantly (figure 3*b*) until just before the funnel. Here the droplets became slightly ellipsoidal, with the long axis approximately parallel to the direction of bulk flow. In whole mounts, it was possible to follow and measure the progressive elongation of these droplets into elongated canaliculi with increasing distance from the start of the duct.

Our observations on the droplets can be used to study elongational flow further. Consider a short cylinder of feedstock with radius r_i, that of the lumen at the start duct and of length l_i. If this undergoes progressive elongation to give a series of cylinders of radius r and length l at any elongation, provided that there is no change in volume, $\pi r_i^2 l_i = \pi r^2 l$. This rearranges to $l/l_i = r_i^2/r^2$ where l/l_i is the elongation at any point. Thus, a straight line fit to the log–log plot of the length of the inclusion against the diameter of the lumen ($R^2 = 0.920$ and $n = 10$; figure 3*b*) indicates that the volume of the feedstock does not change appreciably as it flows through the first two limbs of the duct. It also indicates that the lengthening of the canaliculi results solely from elongational flow in the feedstock matrix surrounding them. The departure of data points for the ampulla from the straight line (figure 3*b*) is thought to result from an increase in volume of the feedstock in this compartment due to secretion by zone B and indicates that here the elongational flow rate must be lower. The observation that the long axis of the elongated inclusions throughout the duct was nearly always parallel to the long axis of the lumen indicates that the flow was laminar and without a separate plug flow (Garg & Kenig 1988). The function of the canaliculi formed in this way is not known but they may act as minute fluid-filled shock absorbers (Fox 1980) to increase the toughness of the thread.

The location and geometry of the draw down taper was investigated in whole mounts. The taper appeared to start in the distal part of the third limb of the duct, $2.45 \pm 0.15\,mm$ ($n = 6$) before the valve, in material fixed immediately after spinning silk at a rate of *ca.* $100\,mm\,s^{-1}$. The feedstock pulled away from the cuticle where the diameter of the lumen narrowed to approximately $20 \pm 2\,\mu m$, smoothly and tapering to give a fibre *ca.* $8\,\mu m$ in diameter at the spigot. A two-stage exponential decay curve showed a close fit ($R^2 = 0.972$ and $n = 36$), to the draw down taper (figure 3*c*). This is of interest because this type of curve has been used to describe the draw down in synthetic polymers (Ginzburg 1993). When the geometries of the hyperbolic duct and draw down taper are compared it is evident that elongational flow rate would be considerably lower in the duct than in the taper.

4. DISCUSSION

Our polarizing micrographs and slow axes plots of the silk feedstock in the second limb of the S-shaped duct show remarkable similarity to the cellular texture described by Bunning & Lydon (1996) in a nematic discotic liquid crystal. They identified this optical texture in the lyotropic system, caesium pentadecafluoro-octanoate–water, but it also known to occur in some thermotropic nematics (Bunning & Lydon 1996). The cellular texture is thought to arise when certain nematic liquid crystals are constrained within narrow glass tubes. Under these conditions, the molecules align epitaxially at the tube's walls but take up a bent configuration in the centre of the tube. This bending results from a thermodynamic minimization in which a small increase in bending energy produces a large reduction in splay energy at the centre of the tube (Bunning & Lydon 1996). The closely similar proportions and geometry of the cellular texture in synthetic systems (Bunning & Lydon 1996) and spider silk feedstock suggest that the elastic constants could be similar in all liquid crystals that exhibit this optical texture. The gradual lengthening of the repeat period in the third limb of the S-shaped duct evident in our preparations may result from flow elongation of the cellular texture (see below). The persistence of an epitaxial molecular alignment at the surface of the final thread after it has been drawn might help to explain the difference in behaviour of coat and core (Vollrath *et al.*

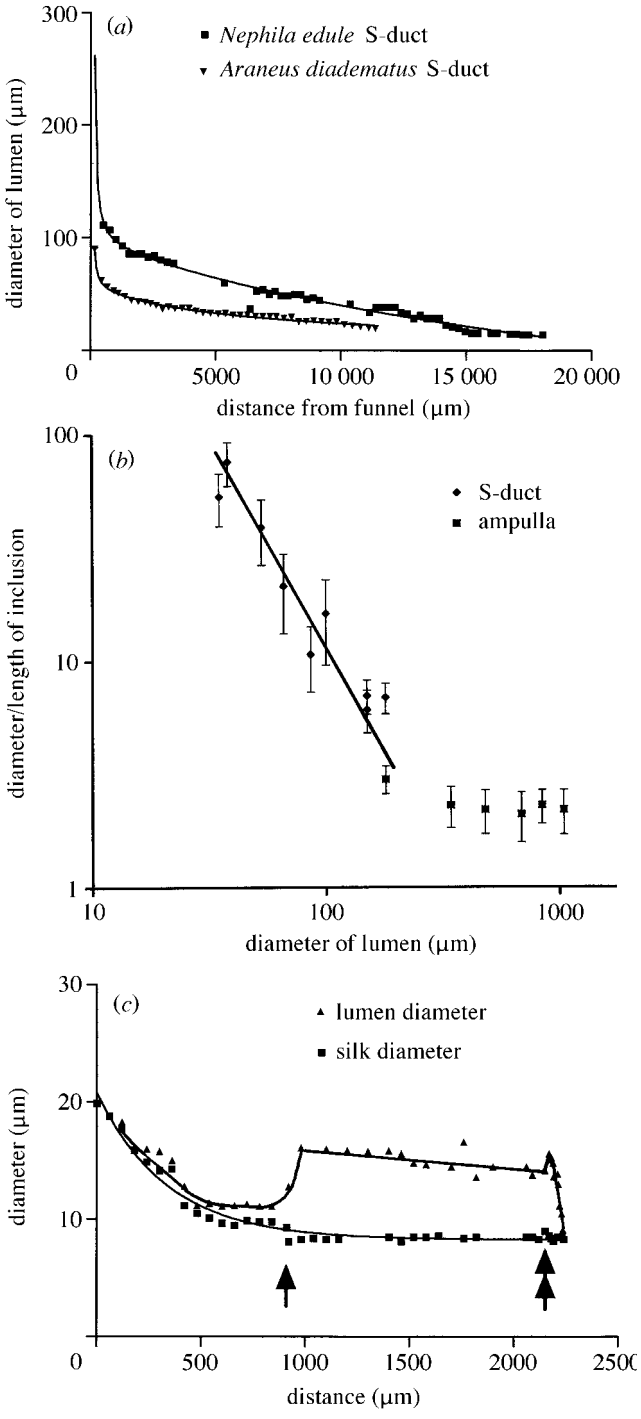

Figure 3. Graphs illustrating aspects of the rheology of silk spinning in the major ampulate gland of *N. edulis*. (*a*) Graph showing changes in the width of the lumen with distance from proximal face of the funnel. A two-stage hyperbolic curve shows a close fit to the profile of both *N. edulis* ($R^2 = 0.979$) and *Araneus diadematus* ($R^2 = 0.989$) ducts. (*b*) Log–log plot of the mean diameter/length ($\pm$s.d.; $n = 20$) of the inclusions in the feedstock against the diameter of the lumen. Only droplets/inclusions in the central part of the lumen were measured because the sizes decreased close to the luminal wall. The plot shows how the inclusions elongate to form the canaliculi seen in the final silk. Data points for the S-shaped duct show a good fit to a straight line indicating that here the granules lengthen by elongational flow without an appreciable change in volume in the feedstock (see text). Departure of data points for the ampulla from the line probably resulted from an increase in volume of the feedstock caused by secretion in zone B and indicates that the elongational flow rate here was less than in the S-shaped duct. (*c*) Graph showing changes in the diameter of the lumen and the silk thread forming in the draw down taper in the distal part of the third limb of the S-shaped duct. The distance along the duct shown on the *x*-axis starts at an arbitrary point just proximal to the start of the draw down taper. The positions of the start of the valve (single arrow) and of the spigot (double arrow) are indicated. A two-stage exponential decay was fitted to the draw down taper ($K_1 = 2.96 \times 10^{-3}$ and $K_2 = 1.78 \times 10^{-4}$).

1996) in super-contracted spider silk. The superficial resemblance of the cellular texture to a double helicoid might account for the helicoidal pattern also described in super-contracted silk by the same authors.

Although we cannot totally rule out the possibility that the cellular texture in silk feedstock is an artefact, we have presented evidence elsewhere that Karnovsky fixation followed by dehydration preserves molecular orientation in another nematic silk feedstock, dogfish egg case collagen (Knight *et al.* 1996, 1997).

The arrangement of nested arcs described above in the silk feedstock within the ampulla of the major ampullate gland could arise by elongational flow (Garg & Kenig 1988) or bending (see above) of a nematic phase within the divergent–convergent geometry (see figure 1*a*) of this part of the secretory pathway. Both hypotheses are compatible with the suggestion of Kerkam *et al.* (1991), based on ultrastructural appearance, that the feedstock is present in the ampulla as a nematic phase. Bending is, however, a more likely explanation as orientation by flow elongation is unlikely at the very slow flow rates suggested by our observations on the behaviour of small droplets in the ampulla (see above).

The hyperbolic geometry of the S-shaped duct described above is of interest. Man-made extrusion dies sometimes use this geometry as it reduces disorientation by maintaining a constant elongational flow rate throughout the entire length of the die (Chen *et al.* 1992). The slow reduction in diameter of the lumen in the spider's ampulla and S-shaped duct are thought to produce a slow elongational flow rate which may prevent premature crystallization of the feedstock until high shear rates (Kerkam *et al.* 1991; Kaplan *et al.* 1994; Willcox *et al.* 1996) are produced in the draw down taper. Elongational flow in the distal part of the duct may help to produce the predominantly axial molecular orientation seen in the feedstock before the start of the draw down taper.

Several changes in texture may occur as the feedstock travels down the secretory pathway. A nematic texture in the ampulla (Kerkam *et al.* 1991) may give rise to a cholesteric phase in the proximal parts of the S-shaped duct (Willcox *et al.* 1996). Our failure to detect this phase by polarized light is not surprising in view of the small repeat period evident in the latter authors' micrographs. The transition from nematic to cholesteric as the feedstock enters the S-shaped duct is unlikely to be driven by changes in water content as our evidence suggests that there is no appreciable change in the feedstock's volume in the first two limbs of the duct. This transition is therefore more likely to be driven by a change in pH (Vollrath *et al.* 1998) and/or the increase in elongational flow rate

indicated by our data on the behaviour of droplets in the feedstock. As the feedstock moves from the first to the second limb of the duct, the cholesteric is thought to transform into the cellular nematic texture. This change may result from the reduction in diameter of the duct. Thereafter, an increase in viscosity (Vollrath *et al.* 1998) coupled with continued flow elongation caused by the convergent geometry is thought to pull out the cellular texture pre-orientating the molecules uniaxially before the start of the draw down taper in the distal part of the third limb. Thereafter, further improvement in the axial alignment is likely to occur as a result of the higher elongation rates in the exponential draw down taper. The small additional draw down (Vollrath & Knight 1998) which occurs after the silk has left the spigot is likely to improve the axial molecular orientation even further. The relatively low elongational flow rates within the ampulla and S-shaped duct may serve to delay formation of the solid thread until considerably higher rates are produced within the draw down taper.

We conclude that dragline silk is produced by the draw down of a pre-orientated liquid crystalline feedstock. Pre-orientation may reduce the viscosity of the feedstock and the energy required to produce an axial alignment of the molecules within the draw down taper and reduce the number of disclinations per unit length of the silk thread, thereby contributing to the exceptional mechanical properties of this material. The spider's manipulation of elongational flow rates of a liquid crystalline feedstock combined with chemical treatment (Vollrath *et al.* 1998) within the secretory pathway may assist the optimal folding of long chain silk proteins (Cappello & McGrath 1994). Thus, liquid crystallinity and flow elongation probably contribute to the extreme toughness and strength of this remarkable material.

We thank John Lydon for identifying our optical texture, Christopher Viney, Xiao Wen Hu, Zhengzhong Shao and Samuel Gido for perceptive comments, the Danish Forskerakademiet and the Danish Statens Naturvidenskabelige Forskningsråd for financial support and Annie Sloth, Else Rasmusen and Julian Haffegee for technical assistance.

REFERENCES

Bunning, J. D. & Lydon, J. E. 1996 The cellular optical texture of the lyotropic nematic phase of the caesium pentadeca-fluoro-octanoate(CsPFO)/water system in cylindrical tubes. *Liquid Crystal.* **20**, 381–385.

Cappello, J. & McGrath, K. P. 1994 Spinning of protein polymer fibers. In *Silk polymers: materials science and biotechnology* (ed. D. Kaplan, W. W. Adams, C. Viney & B. L. Farmer), pp. 311–327. Washington: American Chemical Society.

Chen, G.-Y., Cuculo, J. A. & Tucker, P. A. 1992 Characteristics and design procedure of hyperbolic dies. *J. Polymer Sci. B: Polymer Phys.* **30**, 557–561.

Fox, P. G. 1980 The toughness of tooth enamel, a natural fibrous composite. *J. Materials Sci.* **15**, 3113–3121.

Frische, S., Maunsbach, A. & Vollrath, F. 1997 Elongate cavities and skin-core structure in *Nephila* spider silk observed by electron microscopy. *J. Microscopy*, **189**, 64–70.

Garg, S. K. & Kenig, S. 1988 Development of orientation during the processing of liquid crystalline polymers. In *High modulus polymers: approaches to design and development* (ed. A. E. Zachariades & R. S Porter), pp. 71–104. New York and Basel: Marcel Dekker.

Ginzburg, V. V. 1993 Kinetic-model of fiber drawing. *Polymer* **34**, 5123–5127.

Kaplan, D. L., Adams, W. W., Viney, C. & Farmer, B. L. 1994 *Silk polymers: materials science and biotechnology.* Washington: ACS Books.

Kerkam, K., Viney, C., Kaplan, D. & Lombardi, S. 1991 Liquid crystallinity of natural silk secretions. *Nature* **349**, 596–598.

Knight, D. P., Hu, X. W., Gathercole, L. J., Rusaouën-Innocent, M., Ho, M.-W. & Newton, R. 1996 Molecular orientations in an extruded collagenous composite, the marginal rib of the egg capsule of the dogfish *Scyliorhinus canicula*; a novel lyotropic liquid crystalline arrangement and how it is defined in the spinneret. *Phil. Trans. R. Soc.* B **351**, 1205–1222.

Knight, D. P., Hu, X. W., Newton, R. H., Cipollone, M., Gathercole, L. J. & Koob, T. 1997 Spinnerets in fish extrude sheet material with complex molecular orientations. *J. Biomimetics* **4**, 105–120.

Newton, R. H., Haffegee, J. P. &and Ho, M.-W. 1995 Colour contrast in polarised light microscopy of weakly birefringent biological specimens. *J. Microscopy* **180**, 127–131.

Vollrath, F. & Knight, D. P. 1998 Structure and function of the silk production pathway in the spider *Nephila edulis*. *Int. J. Biol. Macromol.* (In the press.)

Vollrath, F., Holtet, T., Thogersen, H. C. & Frische, S. 1996 Structural organisation of spider silk. *Proc. R. Soc. Lond.* B **263**, 147–151.

Vollrath, F., Knight, D. P. and & Hu, X.W. 1998 Silk production in a spider involves acid bath treatment. *Proc. R. Soc. Lond.* B **265**, 817–820.

Willcox, P. J., Gido, S. P., Muller, W. & Kaplan, D. L. 1996 Evidence of a cholesteric liquid crystalline phase in natural silk spinning processes. *Macromolecules* **29**, 5106–5110.

Wilson, R. S. 1962*a* The control of dragline spinning in the garden spider. *Quart. J. Microscop. Sci.* **103**, 557–571.

Wilson, R. S. 1962*b* The structure of the dragline control valves in the garden spider. *Quart. J. Mmicroscop. Sci.* **103**, 549–555.

Wilson, R. S. 1969 Control of dragline spinning in certain spiders. *Am. Zool.* **9**, 103–111.